ChemComm

COMMUNICATION

View Article Online
View Journal | View Issue

Cite this: *Chem. Commun.*, 2021, **57**, 3897

Received 10th March 2021,
Accepted 16th March 2021

DOI: 10.1039/d1cc01312b

rsc.li/chemcomm

Plug-and-play aqueous electrochemical atom transfer radical polymerization†

Boyu Zhao, Mahir Mohammed, Bryn A. Jones and Paul Wilson *

A simplified 'plug-and-play' approach to aqueous electrochemical atom transfer radical polymerization (eATRP) has been developed. Well-controlled polymerization of $PEGA_{480}$ ($Đ_m$ = 1.17–1.31) is reported under potentiostatic (3-electrodes, undivided cell) and galvanostatic (2-electrodes, 6-steps) conditions.

Recent progress in polymerization methods has advanced to the point where we can exquisitely design and subsequently control polymer synthesis with respect to molecular weight (including dispersity), composition and topology.[1,2] In reversible deactivation radical polymerization (RDRP) (bio)chemical, photochemical,[3] electrochemical,[4] mechanochemical[5] and sonochemical[6] methods have all been developed, enabling external control over the dynamic equilibrium between dormant and active (radical) species, ultimately allowing the overall radical concentration to be accurately controlled.

In Cu-mediated atom transfer radical polymerization (ATRP),[7] the equilibrium (K_{ATRP}) is between dormant alkyl (R-X) or macromolecular (P_n-X) halides and propagating radicals ($R^•/P_n^•$) that undergo reversible redox reactions with Cu-complexes. The redox nature of the ATRP mechanism lends itself to electrochemical manipulation and control.[4,8] The active, yet oxidatively labile $Cu^{I}L$ complex can be formed *in situ* when a potential is applied (E_{app}) to promote a one electron reduction of an inactive $Cu^{II}L$ precursor. The equilibrium between dormant and active species (K_{ATRP}), and the kinetics of polymerization, can therefore be controlled by tuning the potential of the system. Thus, electrochemical ATRP (eATRP) has been demonstrated to provide high fidelity on–off temporal control over polymer synthesis in solution for a variety of polymer architectures,[9,10] in dispersed media[11] and from surfaces (si-eATRP).[12]

A perceived limitation of the original eATRP reactions was the complexity of the reaction set-up. A 3-electrode divided electrochemical cell was used with reactions carried out under potentiostatic (constant potential) conditions to avoid unwanted side-reactions occurring at the counter electrode (anode). This was alleviated by the development of simplified eATRP (seATRP), which employs a sacrificial counter electrode as the anode.[13] For example, aluminum wire has been employed for the synthesis of linear and star-like polymers *via* seATRP with the Al-wire, and the products of its oxidation (Al^{3+}), being inert to the eATRP reaction conditions.[14–21] Thus, seATRP reaction conditions allow undivided cells to be used in 3-electrode configurations (potentiostatic). Furthermore, reactions can be run in a 2-electrode configuration under galvanostatic conditions (constant current) using a simple (and cheaper) current generator in place of a potentiostat.

The complexity of electrosynthetic reaction set up is not unique to eATRP. In organic electrosynthesis and electrocatalysis the reaction set up, from electrode materials to cell configuration has historically been viewed as a black-box which has limited wide-spread application of electrolysis to solve synthetic problems.[22] This perspective has dramatically changed recently due to the development and reporting of standardized hardware and reaction conditions.[23,24] For example, the IKA Electrasyn device, which is a magnetic stirring plate with an in-built potentiostat allows both constant current and potential reactions to be performed.[25] With a range of standardized electrodes and other accessories, this has transformed electrosynthesis into almost a 'plug-and-play' methodology that is accessible to the entire synthetic community.

Thus, we were interested to see if further simplification of eATRP using these 'plug-and-play' features could be achieved. Although a number of seATRP reactions in organic solvents[14–21] have been reported, the number of aqueous reactions reported is more limited.[26,27] With this in mind, we opted to investigate whether aqueous seATRP of poly(ethylene glycol) methyl ether acrylate (M_n = 480; $PEGA_{480}$) could be achieved using the capabilities afforded by the Electrasyn device.

Initially, cyclic voltammetry (CV) of the Cu-complex (Cu^{II}/TPMA) was performed in solutions of the reaction mixture (10% (v/v) $PEGA_{480}$ in H_2O) in the absence and presence of the

Department of Chemistry, University of Warwick, Coventry, CV4 7AL, UK.
E-mail: p.wilson.1@warwick.ac.uk

† Electronic supplementary information (ESI) available. See DOI: 10.1039/d1cc01312b

Table 1 Effect of applied potential (E_{app}) on the seATRP of PEGA (10% v/v, unless stated otherwise) in H_2O. [$PEGA_{480}$] : [HEBiB] : [$Cu(OTf)_2$] : [TPMA] : [NaBr] = [38] : [1] : [0.15] : [0.45] : [0.15]

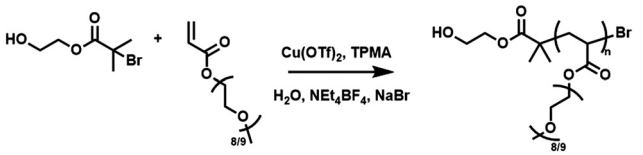

Entry	E_{app}/V	Time/h	Conv.[e]/%	$M_{n,th}$[f]/g mol^{-1}	$M_{n,SEC}$[g]/g mol^{-1}	$Đ_m$[g]
1	−0.2	8	73	13 526	11 000	1.25
2	−0.15	8	54	10 100	9200	1.17
3	−0.25	8	63	11 337	12 900	1.33
4	−0.3	4.5	49	9149	8800	1.52
5	−0.35	4	50	9331	8900	1.71
6[a]	−0.2	8	84	15 532	13 700	1.41
7[b]	−0.2	8	86	15 897	11 910	1.61
8[c]	−0.2	8	50	9331	8600	2.56
9[a]	−0.15	8	65	12 067	14 900	1.23
10[b]	−0.15	8	83	15 350	14 500	1.31
11[c]	−0.15	8	76	14 073	16 500	1.41
12[d]	−0.15	8	23	4406	6100	3.28

[a] [$PEGA_{480}$] = 20% v/v. [b] [$PEGA_{480}$] = 30% v/v. [c] [$PEGA_{480}$] = 40% v/v. [d] [$PEGA_{480}$] = 50% v/v. [e] Determined *via* ^{1}H NMR of reaction samples performed in D_2O. [f] $M_{n,th}$ = [(conv./100 × $DP_{n,th}$) × 480] + 221. [g] From THF SEC of purified polymers.

initiator, hydroxyethyl-2-bromoisobutyrate (HEBiB) (Fig. S1, ESI†). The expected [Cu^{II}/TPMA]/[Cu^{I}/TPMA] redox process was observed and the standard reduction potential ($E^{\theta} \approx E_{1/2} = E_{pc} + E_{pa}/2$) was found to be −0.197 V (*vs.* Ag/AgCl). Upon addition of HEBiB the intensity of E_{pc} increased while the intensity of E_{pa} decreased significantly indicative of electrochemical reduction of [Cu^{II}/TPMA] to [Cu^{I}/TPMA] followed by rapid activation of HEBiB by the [Cu^{I}/TPMA].

Potentiostatic reactions, performed in undivided cells, were investigated first using a Pt-coated working electrode (IKA), Al-wire counter electrode and a Ag/AgCl reference (Fig. S2 and S3, ESI†). Based on $E^{\theta} \approx E_{1/2} = -0.197$ V, seATRP was initially performed with using [$PEGA_{480}$] : [HEBiB] : [$Cu(OTf)_2$] : [TPMA] : [NaBr] = [38] : [1] : [0.15] : [0.45] : [0.15] with E_{app} = −0.20 V (Table 1, entry 1). The polymerization was following by ^{1}H NMR and conversion was determined *via* integration of one the vinyl protons (H_f) against the methylene protons (H_c) adjacent to the ester group of the $PEGA_{480}$ monomer and emerging polymer (Fig. S4, ESI†). Kinetic analysis of the reaction revealed pseudo-first order kinetics (Fig. 1A), reaching 73% conversion after 8 h. The evolution of molecular weight with conversion was followed by SEC (Fig. 1C and Fig. S5, ESI†) and found to be linear, as expected for RDRP. The purified polymer ($PPEGA_{480}$) had a number average molecular weight; $M_{n,SEC}$ = 11 000 g mol^{-1}, which was in good agreement to the theoretical value ($M_{n,th}$ = 13 526 g mol^{-1}), and a relatively low dispersity ($Đ_m$ = 1.25).

To investigate the effect of E_{app} in our 'plug-and-play' configuration, reactions were repeated at ±0.05 V increments. At less reducing potentials (E_{app} = −0.15 V, Table 1, entry 2) the polymerization was under better control furnishing $PPEGA_{480}$ with lower final dispersity ($Đ_m$ = 1.17). However, at more reducing potentials (E_{app} = −0.25 to −0.35 V, Table 1, entries 3–5) the dispersities of the final polymers gradually increased ($Đ_m$ = 1.33–1.72). These observations are in agreement with the previous literature[28] and the proposed relationship between E_{app} and ratio of [Cu^{I}] and [Cu^{II}] present in the reaction, as described by the Nernst equation.

Kinetic analysis was also performed for the polymerizations at $E_{app} = E_{1/2} \pm 0.05$ V. The gradient of the linear region of the kinetic plots revealed an apparent rate constant for propagation, k_p^{app} = 0.21 h^{-1} when E_{app} = −0.15 V. This increased to k_p^{app} = 0.24 h^{-1} when $E_{app} = E_{1/2}$ = −0.20 V and k_p^{app} = 0.26 h^{-1} at E_{app} = −0.25 V (Fig. 1B). All three polymerizations proceeded with a linear evolution of $M_{n,SEC}$ with conversion (Fig. 1C). Deviations in $M_{n,SEC}$ from $M_{n,th}$, are likely due to errors caused by overlap of the monomer and emerging polymer peaks in the SEC chromatographs of the reaction samples (Fig. S5, ESI†).

The effect of monomer concentration was then investigated at E_{app} = −0.20 V and E_{app} = −0.15 V. Increasing the [$PEGA_{480}$] to 20% and 30% (v/v) resulted in increased conversions of 84% and 86% when E_{app} = −0.20 V (Table 1, entries 6 and 7). However, the polymerizations were not as well controlled producing polymers with $Đ_m$ = 1.41 and 1.61 respectively. Increasing [$PEGA_{480}$] further to 40% v/v resulted in only 50% conversion and $Đ_m$ > 2.5 indicating that the reaction was completely uncontrolled (Table 1, entry 8). When E_{app} = −0.15 V, increasing [$PEGA_{480}$] to 20% and 30% (v/v) had a similar effect. The

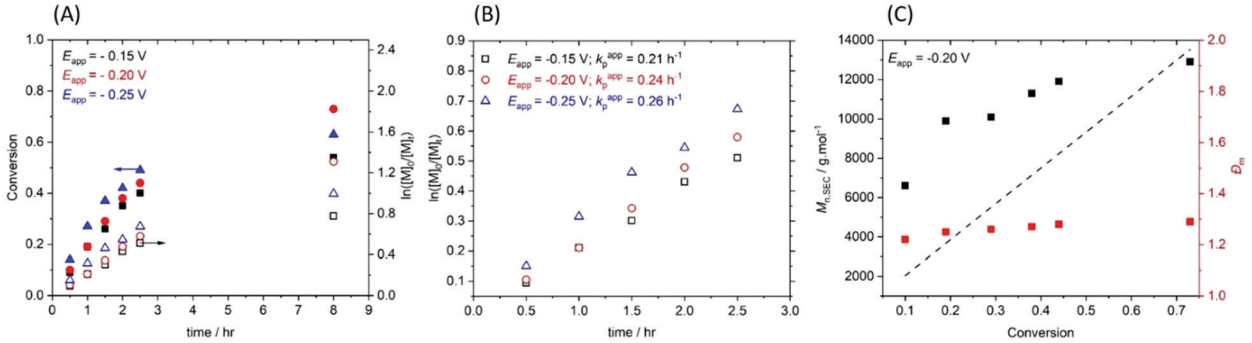

Fig. 1 For [$PEGA_{480}$] : [HEBiB] : [$Cu(OTf)_2$] : [TPMA] : [NaBr] = [38] : [1] : [0.15] : [0.45] : [0.15]; (A) conversion and pseudo first order kinetic plots as a function of E_{app}. (B) A zoom in the region between t = 0–2.5 h from which k_p^{app} was determined. (C) Evolution of the $M_{n,SEC}$ and $Đ_m$ with conversion (E_{app} = −0.20 V).

conversion increased to 65% and 83% respectively (Table 1, entries 9 and 10). In this case the control over the polymerizations was retained ($Đ_m < 1.31$). Increasing the [$PEGA_{480}$] further to 40% and 50% (v/v) led to the conversion decreasing to the 76% and 23% respectively, and control over the polymerizations being compromised ($Đ_m$ = 1.41–3.28, Table 1, entries 11 and 12). The gradual increase in $Đ_m$ can be attributed to the gradual increase in termination reactions, manifest as the emergence of high molecular weight shoulder peaks in the SEC chromatograms as [$PEGA_{480}$] is increased from 20–40% (v/v) (Fig. S6, ESI†). This is exacerbated at 50% (v/v) where significant high molecular weight tailing was observed leading to $Đ_m$ = 3.28.

Based on conversion, kinetics and $Đ_m$ reported in Table 1, subsequent polymerizations targeting $PPEGA_{480}$ with different $DP_{n,th}$ were performed at E_{app} = −0.15 V for 2.5 h. Repeating the polymerization for [$PEGA_{480}$]:[HEBiB] = [38]:[1] resulted in 53% conversion and final polymer with and $M_{n,SEC}$ (11 600 g mol^{-1}) in good agreement with $M_{n,th}$ (9878 g mol^{-1}) and a low dispersity ($Đ_m$ = 1.17) (Table 2, entry 2). Decreasing [$PEGA_{480}$]:[HEBiB] to [19]:[1] led to higher conversion (68%) after 2.5 h (Table 2, entry 1).

However, a slightly higher dispersity ($Đ_m$ = 1.21) and deviation in $M_{n,SEC}$ (9100 g mol^{-1}) and $M_{n,th}$ (6412 g mol^{-1}) was observed. Increasing [$PEGA_{480}$]:[HEBiB] to [57]:[1], [76]:[1] and [114]:[1] resulted in conversions between 45–55% within 2.5 h (Table 2, entries 3–5). The final polymers all exhibited good agreement between $M_{n,SEC}$ and $M_{n,th}$ and low $Đ_m$ indicative of well controlled polymerizations. An overlay of the SEC chromatograms shows the gradual shift to higher molecular weight as a function of increasing [$PEGA_{480}$]:[HEBiB] (Fig. S7, ESI†).

The temporal control afforded by standard eATRP reactions was then investigated in an experiment wherein E_{app} = −0.15 V was switched on and off for 30 min intervals during the course of a reaction (Fig. 2). During step 1 (t_{ON} = 0.5 h, $k_p^{app,1}$ = 0.71 h^{-1}) 30% conversion was obtained. At this point the E_{app} was set to 0 V and the reaction was left for a further 30 min during which no further polymerization was observed. During step 2 (E_{app} = −0.15 V) polymerization restarted, albeit at a slightly slower rate ($k_p^{app,2}$ = 0.48 h^{-1}), reaching 45% conversion (t_{ON} = 1 h). Again polymerization was halted upon removal of E_{app} and restarted again after 30 min. Conversion increased to 56% (Step 3, t_{ON} = 1.5 h, k_p^{app} = 0.45 h^{-1}) before E_{app} was switched off for a third and final 30 min period. E_{app} was switched back on and the polymerization was allowed to proceed for a further 6.5 h (t_{ON} = 8 h in total), resulting in a final conversion of 73% (Fig. S8A, ESI†). Molecular weight analysis of the final polymer revealed a $M_{n,SEC}$ = 22 900 g mol^{-1} which is higher than expected ($M_{n,th}$ = 13 526 g mol^{-1}), indicating that some active chain-ends were lost during these polymerizations. Evidence for this was not apparent in the symmetrical SEC chromatogram and the final dispersity ($Đ_m$ = 1.28) indicated that good control was retained (Fig. S8B, ESI†).

Finally, the polymerization of $PEGA_{480}$ was attempted in a 2-electrode set up under galvanostatic conditions (constant current). Conveniently, during potentiostatic reactions (*vide supra*), the IKA Electrasyn (*via* a bespoke mobile app) records current (*I*) *vs.* time graphs which can be integrated to determine the total charge passed during a reaction (*Q*). This can be used to determine the applied currents (I_{app}) for subsequent galvanostatic reactions. The current *vs.* time plot (Fig. 3A) contains two distinct regimes. With reference to the mechanism, the initial current decay regime can be explained by the reduction of Cu^{II}/L to Cu^{I}/L at the Pt-cathode, coupled to activation of R-X/P_n-X by Cu^{I}/L to form $R^•$/$P_n^•$ and Cu^{II}/L in the bulk. The constant current regime that follows is therefore indicative of

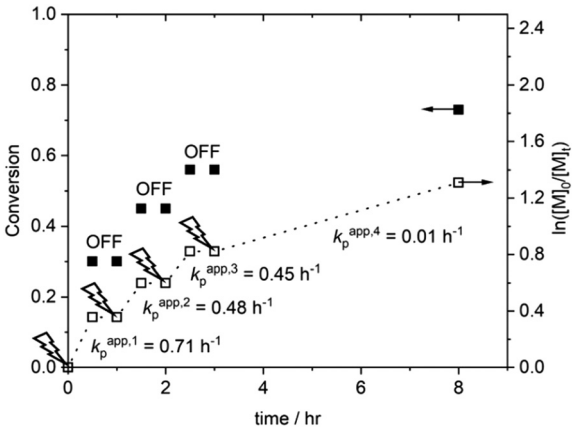

Fig. 2 Conversion and pseudo first order kinetic plot demonstrating temporal control afforded by eATRP in the ‚plug-and-play configuration. [$PEGA_{480}$] : [HEBiB] : [$Cu(OTf)_2$] : [TPMA] : [NaBr] = [38] : [1] : [0.15] : [0.45] :[0.15]; E_{app} = −0.15 V.

Table 2 Effect of applied potential E_{app} on the seATRP of PEGA (10% v/v, unless stated otherwise) in H_2O. [$PEGA_{480}$] : [HEBiB] : [$Cu(OTf)_2$] : [TPMA] : [NaBr] = [38] : [1] : [0.15] : [0.45] : [0.15]

Entry	[M]/[I]	Time/h	Conv.[a]/%	$M_{n,th}$[b]/g mol^{-1}	$M_{n,SEC}$[c]/g mol^{-1}	$Đ_m$[c]
1	19	2.5	68	6412	9100	1.21
2	38	2.5	53	9878	11 600	1.17
3	57	2.5	54	14 985	16 100	1.28
4	76	2.5	55	20 275	18 900	1.21
5	114	2.5	45	24 835	19 300	1.32

[a] Determined *via* ^{1}H NMR of reaction samples performed in D_2O. [b] $M_{n,th}$ = [(conv./100 × $DP_{n,th}$) × 480] + 221. [c] From THF SEC of purified polymers.

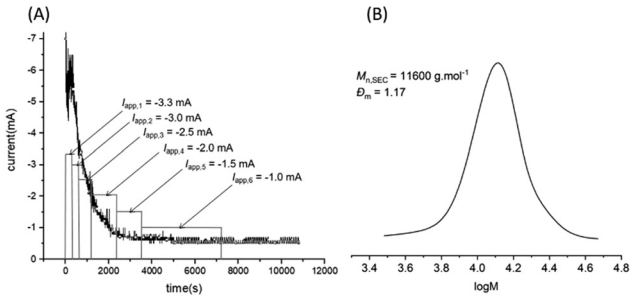

Fig. 3 (A) *I vs.* time plot obtained during a potentiostatic reaction when [$PEGA_{480}$] : [HEBiB] : [$Cu(OTf)_2$] : [TPMA] : [NaBr] = [38] : [1] : [0.15] : [0.45] : [0.15]; E_{app} = −0.15 V. (B) SEC chromatogram of the purified polymer obtained from the polymerization performed using the 2-electrode, galvanostatic configuration with [$PEGA_{480}$] : [HEBiB] : [$Cu(OTf)_2$] : [TPMA] : [NaBr] = [38] : [1] : [0.15] : [0.45] : [0.15]; I_{app} can be found in Table S2 (ESI†).

equilibrium being reached and the concentration of each component, particularly Cu^{I}/L, reaching steady state. Based on the this, and previous reports,[13] a 4-step current profile (−3.3 mA to −0.3 mA, 180 min, Table S1, entry 1, ESI†) was attempted which yielded 60% conversion and a final $PPEGA_{480}$ with good agreement between experimental ($M_{n,SEC}$ = 10 900 g mol^{-1}) and theoretical ($M_{n,th}$ = 11 154 g mol^{-1}) molecular weights.

However, a relatively high dispersity ($Đ_m$ = 1.51) suggested that the polymerization was not well controlled. According to Ohm's law, in galvanostatic reactions, the potential changes in order to maintain constant current. During our reactions we observed, *via* the user interface, that the (unreferenced) potential gradually became more reducing during the course of these reactions. In our potentiostatic reactions, $E_{app} < -0.25$ V had a detrimental effect on the outcome of the polymerizations (*vide supra*). With this in mind we developed a 6-step current profile (−3.3 mA to −0.3 mA, 120 min, Tables S1, entry 2 and S2, ESI†) to minimize the drift in the potential. These conditions gave an almost identical outcome to the potentiostatic reactions yielding $PPEGA_{480}$ in 55% conversion with good agreement between experimental ($M_{n,SEC}$ = 11 600 g mol^{-1}) and theoretical ($M_{n,th}$ = 10 243 g mol^{-1}) molecular weights and low dispersity ($Đ_m$ = 1.17, Fig. 3B)

In conclusion, a new simplified approach to eATRP has been demonstrated using the 'plug-and-play' capabilities afforded by the IKA Electrasyn device. Well controlled $PPEGA_{480}$ has been synthesized under potentiostatic conditions (3-electrodes, undivided cell) with conversions up to 83%, good agreement between $M_{n,SEC}$ and $M_{n,th}$ and relatively low dispersities ($Đ_m$ = 1.17–1.31). Likewise, a polymerization performed under galvanostatic conditions (2-electrodes, 6-step profile) has been shown to afford very similar polymers, with good agreement between $M_{n,SEC}$ and $M_{n,th}$ and low dispersity ($Đ_m$ = 1.17). The availability of a range of standardized, manufactured electrodes as well as accessories that support *e.g.* variable temperatures, parallel and flow reactions, offers great potential for optimization and further development of this seATRP methodology. Ultimately, it could make eATRP more accessible to the polymer chemistry and materials science communities and the simplicity of the hardware and reaction set-up is even amenable to translation into undergraduate teaching laboratories.

The authors would like to thank the Polymer Characterization and Microscopy Research Technology Platforms for maintenance, access and use of SEC, DLS and TEM facilities. P. W. thanks the Royal Society and Tata companies for the award of a University Research Fellowship (URF\R1\180274). P. W. also thanks the EPSRC for funding a DTP studentship (M. M. EP/R513374/1).

Conflicts of interest

There are no conflicts to declare.

Notes and references

1 K. Parkatzidis, H. S. Wang, N. P. Truong and A. Anastasaki, *Chemistry*, 2020, **6**, 1575–1588.
2 N. Corrigan, K. Jung, G. Moad, C. J. Hawker, K. Matyjaszewski and C. Boyer, *Prog. Polym. Sci.*, 2020, **111**, 101311.
3 B. P. Fors and C. J. Hawker, *Angew. Chem., Int. Ed.*, 2012, **51**, 8850–8853.
4 A. J. D. Magenau, N. C. Strandwitz, A. Gennaro and K. Matyjaszewski, *Science*, 2011, **332**, 81–84.
5 H. Y. Cho and C. W. Bielawski, *Angew. Chem., Int. Ed.*, 2020, **59**, 13929–13935.
6 H. Mohapatra, M. Kleiman and A. P. Esser-Kahn, *Nat. Chem.*, 2017, **9**, 135–139.
7 X. Pan, M. Fantin, F. Yuan and K. Matyjaszewski, *Chem. Soc. Rev.*, 2018, **47**, 5457–5490.
8 P. Chmielarz, M. Fantin, S. Park, A. A. Isse, A. Gennaro, A. J. D. Magenau, A. Sobkowiak and K. Matyjaszewski, *Prog. Polym. Sci.*, 2017, **69**, 47–78.
9 S. Park, H. Y. Cho, K. B. Wegner, J. Burdynska, A. J. D. Magenau, H.-J. Paik, S. Jurga and K. Matyjaszewski, *Macromolecules*, 2013, **46**, 5856–5860.
10 P. Chmielarz, *eXPRESS Polym. Lett.*, 2017, **11**, 140–151.
11 M. Fantin, S. Park, Y. Wang and K. Matyjaszewski, *Macromolecules*, 2016, **49**, 8838–8847.
12 B. Li, B. Yu, W. T. S. Huck, F. Zhou and W. Liu, *Angew. Chem., Int. Ed.*, 2012, **51**, 5092–5095.
13 S. Park, P. Chmielarz, A. Gennaro and K. Matyjaszewski, *Angew. Chem., Int. Ed.*, 2015, **54**, 2388–2392.
14 P. Chmielarz, *Chem. Pap.*, 2017, **71**, 161–170.
15 P. Chmielarz, *Polymer*, 2016, **102**, 192–198.
16 P. Chmielarz, S. Park, A. Sobkowiak and K. Matyjaszewski, *Polymer*, 2016, **88**, 36–42.
17 P. Chmielarz, A. Sobkowiak and K. Matyjaszewski, *Polymer*, 2015, **77**, 266–271.
18 P. Chmielarz, *Polym. Adv. Technol.*, 2017, **28**, 1787–1793.
19 P. Chmielarz, *Polym. Adv. Technol.*, 2018, **29**, 470–480.
20 P. Chmielarz, T. Pacześniak, K. Rydel-Ciszek, I. Zaborniak, P. Biedka and A. Sobkowiak, *Beilstein J. Org. Chem.*, 2017, **13**, 2466–2472.
21 P. Chmielarz and A. Sobkowiak, *J. Polym. Res.*, 2017, **24**, 77.
22 M. Yan, Y. Kawamata and P. S. Baran, *Angew. Chem., Int. Ed.*, 2018, **57**, 4149–4155.
23 C. Schotten, T. P. Nicholls, R. A. Bourne, N. Kapur, B. N. Nguyen and C. E. Willans, *Green Chem.*, 2020, **22**, 3358–3375.
24 M. Yan, Y. Kawamata and P. S. Baran, *Chem. Rev.*, 2017, **117**, 13230–13319.
25 C. Kingston, M. D. Palkowitz, Y. Takahira, J. C. Vantourout, B. K. Peters, Y. Kawamata and P. S. Baran, *Acc. Chem. Res.*, 2020, **53**, 72–83.
26 F. De Bon, S. Marenzi, A. A. Isse, C. Durante and A. Gennaro, *ChemElectroChem*, 2020, **7**, 1378–1388.
27 M. Fantin, F. Lorandi, A. A. Isse and A. Gennaro, *Macromol. Rapid Commun.*, 2016, **37**, 1318–1322.
28 A. Michieletto, F. Lorandi, F. De Bon, A. A. Isse and A. Gennaro, *J. Polym. Sci.*, 2020, **58**, 114–123.

